

# Coherent WDM Systems Using in-Line Semiconductor Optical Amplifiers

Amirhossein Ghazisaeidi

**Abstract**—A theory of nonlinear signal propagation in multi-span wavelength division multiplexed coherent transmission systems that employ the semiconductor optical amplifier as in-line amplifiers is presented for the first time. The rigorous derivation, based on time-domain first-order perturbation theory, is developed in detail. The end result is the expressions for the signal-to-noise ratio of the received sampled photocurrent, including contributions from noise, fiber-induced nonlinear distortions, and amplified-induced nonlinear distortions.

**Index Terms**—Nonlinear impairments, in-line semiconductor optical amplifier, coherent WDM, perturbation theory.

## I. INTRODUCTION

RECENT years have witnessed the combination of some advanced techniques, such as high cardinality shaped constellations, single-channel digital nonlinear compensation, and adaptive-rate capacity approaching forward error correction codes, to boost the spectral efficiency and the throughput of coherent wavelength division multiplexed (WDM) multi-span single-mode fiber-optic transmission systems. [1]- [4]. The spectral efficiency of fiber-optic transmission systems is fundamentally limited by fiber nonlinear impairments [5], [6]. Single-channel nonlinear compensation cannot mitigate nonlinear interference stemming from the adjacent channels. Multi-channel nonlinear compensation is prohibitively complex; moreover, in meshed networks the adjacent channels are added and dropped along the optical path of the channel of interest (COI); therefore, the received samples of the adjacent channel might not be adequate for the multi-channel nonlinear equalizer to efficiently mitigate nonlinear impairments. Even if the complexity is not a concern, and all the adjacent channels are perfectly known and jointly processed at the receiver, the nonlinear interaction between signal and spontaneous emission noise (ASE), an effect which will be referred to as NSNI in this work, sets the fundamental upper limit on the achievable spectral efficiency using the standard digital backpropagation (DBP) nonlinear equalizer. In [7] we have studied those fundamental limits, and demonstrated that the maximum improvement in spectral efficiency of conventional coherent WDM systems using full-field DBP is about 50-60%.

Besides nonlinearity, the throughput of conventional WDM systems is also limited by the total bandwidth of erbium-doped fiber amplifiers (EDFA). Recent experiments using C+L dual-band EDFAs have an optical transmission bandwidth about 9 THz [1]- [4]. In order to extend the transmission bandwidth, all-Raman in-line amplification might be used [8], [9], but it has its own drawbacks, most importantly the distributed nature

of all-Raman amplification, which is hardly compatible with routed networks topology, and its low power efficiency. Note that even if all-Raman amplification is a viable option for *in-line* amplifications, transmitter-side boosters and receiver-side pre-amplifiers are still EDFAs in [8], [9].

Another alternative to EDFA and Raman optical amplification schemes is semiconductor optical amplifiers (SOA) [10]. It has been shown that SOAs can deliver amplification bandwidths up to 120 nm [11]. The SOA consists of an electronically pumped millimeter-long active waveguide, and is an integrable device providing lumped gain, thus, it is an attractive potential candidate for replacing in-line amplifiers, boosters and pre-amplifiers in a multi-span repeated transmission system. However, light amplification by the SOA is a nonlinear process; the gain fluctuates dynamically, at the nanosecond scale, in response to input signal intensity fluctuations; moreover, the typical noise figure (NF) of the SOA is around 7 dB or higher, whereas that of modern EDFAs is around to 4-5 dB. Due to its nonlinear behavior and high NF, the SOA has not been used as an in-line amplifier in the past. In fact, most of the versatile applications of the SOA are based on exploiting its nonlinear behavior in order to realize various optical signal processing functions [10].

In September 2017, Renaudier *et al.* have demonstrated the first coherent WDM transmission system employing custom-designed in-line ultra-wideband SOAs, with more than 100 nm continuous optical amplification band instead of EDFAs, with improved nonlinear and noise performance [12]. This new result may pave the way for novel SOA-based coherent WDM systems with considerable throughput increase with respect to the present-day EDFA-amplified systems. That demonstration is the main motivation of the present work, where, we present for the first time, a rigorous theory of nonlinear signal propagation in coherent WDM multi-span systems based on in-line SOAs. Note that although a vast literature exist on modeling the SOA device *per se*, as well as for various optical signal processing applications (cf. below for more details), transmission systems with in-line SOA amplifiers have not been studied in the literature due to the above mentioned lack of motivation. To the author's knowledge, the only exception is the numerical investigations in [13].

Nonlinear signal propagation in EDFA-based coherent WDM systems has been extensively studied [7], [14]- [18]<sup>1</sup>. Nonlinear propagation in Raman-amplified systems is addressed in [19]. In particular, in [7] we have presented a detailed demonstration of time-domain perturbative approach

<sup>1</sup>This list is not exhaustive by far. For a detailed discussion of various approaches to modeling nonlinear signal propagation in coherent systems cf. the introduction section of [7] and the references therein.

A. Ghazisaeidi is with Nokia Bell Labs, Paris-Saclay, Route de Villejust, 91620, Nozay, France e-mail: (amirhossein.ghazisaeidi@nokia-bell-labs.com).

to nonlinear wave propagation in EDFA-based coherent systems, first proposed in [14]. In [7], both signal-signal (SS) and noise-signal (NS) nonlinear distortions have been rigorously studied, and the signal-to-noise ratio (SNR) of the received sampled signals are computed with and without nonlinear compensation. The departure point of the present work is [7]. For the sake of simplicity, we limit our analysis to single-polarization fields and ignore the NSNI. We replace EDFAs by SOAs, and follow the lines of [7]. We introduce necessary modifications to the theory, due to the presence of the gain dynamics of the SOAs, and compute the variance of total nonlinear SS distortions of the sampled received signal.

The main new ingredient of the present work is the SOA model. An extensive literature on modeling the behavior of the SOA exists (cf. [20]- [24] and the references therein for a non-exhaustive literature review). On one extreme there exist very sophisticated space-resolved models with tens of parameters that allow for accurate modeling most of the optical and electrical physical processes inside the SOA, *e.g.*, the space-dependence of material gain and optical field inside the SOA waveguide, forward and backward propagation, frequency dependence of gain and other parameters, various radiative and non-radiative recombination processes *etc.*, and are suitable for in-depth studies of the device physics [21]. On the other extreme, there are very simple reservoir models, containing only few parameters, yet successfully capturing the main features of the gain dynamics of the SOA, and so are more useful for system studies where SOAs are combined with many other components in a system architecture [20]. In past, we have used the reservoir model of [20] to study the statistical properties of SOA nonlinear noise [25]- [27], the nonlinear patterning effect in the SOA [28], and digital post-compensation of SOA nonlinearity [29], [30], and have found satisfactory match with experimental data. In this paper we adopt the model presented in [20] for the in-line SOAs in the multi-span coherent WDM systems, and derive expressions for the SNR of the sampled received signal, using the time-domain first-order regular perturbation theory (FRP), following the steps of [7].

The structure of the paper is as follows. In Section II we present the theory. Section II.A is devoted to the basic definitions and problem statement, In section II.B the SOA model is presented, In section II.C. The perturbative analysis of the gain dynamics is presented in II.D. In section II.E the full perturbative analysis of the whole system is presented. In II.F the zeroth order solutions are derived. In II.G the sampled photocurrent at the receiver side is analyzed, and in section II.H the variance of nonlinear distortions are computed. In section III conclusions are drawn. The mathematical background is covered in Appendix A, whereas the detailed derivation of the variance of the SOA-induced nonlinear distortions is presented in Appendix B.

## II. THEORY

### A. Basic definitions

We consider a multi-span coherent WDM transmission system, with an SOA at the end of each span, as illustrated

in Fig. 1.a. In [7] we presented a detailed analysis of the EDFA-based multi-span coherent WDM systems, assuming polarization multiplexed signals, and computed the variance of nonlinear signal-signal (SS) and noise-signal (NS) distortions of the sampled received signals of the channel of interest (COI). In this work, we consider single polarization, replace EDFAs by SOAs, and calculate the variance of SS distortions, using first-order regular perturbation (FRP). We adopt exactly the same notation as in [7], except for variables and parameters related to modeling the optical amplifiers, where the notations for the amplifier gain are more elaborate than [7], and new symbols for the SOA physical parameters are introduced. Table I lists the definition of basic variables and parameters used in this work. If a symbol/notation is not explicitly defined in the text, it should be looked up in Table I. For convenience, we have collected the basic mathematical definitions and identities, required throughout the paper in Appendix A.

The equivalent baseband total optical field envelop at TX output is (cf. Table I and Fig. 1)

$$E(0, t) = \sum_k a_k A_k(0, t) + \sum_{k, s \neq 0} a_{k, s} A_{k, s}(0, t - \delta T_s) \exp[-i\Omega_s t + i\phi_s(0)]. \quad (1)$$

Note that  $A_k(z, t) = A_0(z, t - kT)$ . We assume the pulse shape of all WDM channels is the ideal Nyquist pulse, with roll-off 0 and energy  $\mathcal{E} = PT$ , *i.e.*,

$$\mathcal{E} = \int_{-\infty}^{+\infty} |A_0(0, t)|^2 dt. \quad (2)$$

We will sometimes work with the power normalized pulse-shape  $U_0(z, t) = A_0(z, t)/\sqrt{\mathcal{E}}$  in the sequel.

### B. SOA model

We assume all SOAs are identical components, and adopt the model proposed in [20]. In this section we suppose that the SOAs are noiseless. The ASE source, will be added later to the propagation equation (cf.(15)). In this work we do not study the nonlinear interaction between signal and ASE noise neither in fiber nor in SOA. The  $n^{\text{th}}$  SOA is placed at the end of the  $n^{\text{th}}$  span, and extends from  $z = z_n$  to  $z = z_n + l$ . Inside the SOA waveguide cavity, *i.e.*, for  $z_n \leq z \leq z_n + l$ , the material gain coefficient of the  $n^{\text{th}}$  amplifier,  $g_n(z, t)$ , satisfies the following equation

$$\tau_c \partial_t g_n(z, t) = g_o - g_n(z, t) - g_n(z, t) \frac{|E(z, t)|^2}{P_{sat}}. \quad (3)$$

In this work, we denote the reciprocal of the saturation power of the SOA by  $\epsilon$ . We have

$$\epsilon = \frac{1}{P_{sat}} \quad (4)$$

The field entering the  $n^{\text{th}}$  amplifier is  $E(z_n, t)$ . Inside the  $n^{\text{th}}$  amplifier,  $z_n \leq z \leq z_n + l$ , the following propagation equation holds

$$\partial_z E(z, t) = \frac{1}{2}(1 - i\alpha_H)g_n(z, t)E(z, t). \quad (5)$$

TABLE I  
DEFINITION OF THE BASIC SYMBOLS AND NOTATIONS

$c$	speed of light [m/s]	$\alpha$	fiber loss coefficient [1/m]
$\hbar$	Planck constant divided by $2\pi$ [Js]	$\beta_2$	fiber group velocity dispersion coefficient [ $s^2/m$ ]
$t$	time [s]	$\gamma$	fiber Kerr nonlinear coefficient [1/W/m]
$f$	frequency [Hz]	$n_{sp}$	SOA population inversion factor
$\omega$	angular frequency [rad./s]	$P_{sat}$	SOA saturation power [W]
$\omega_0$	center angular frequency [rad./s]	$\tau_c$	SOA carrier lifetime [s]
$\lambda_0$	center wavelength [nm]	$\alpha_H$	SOA linewidth enhancement factor
$z$	spatial coordinate along propagation direction [m]	$l$	cavity length of the SOA [m]
$z_0$	coordinate of the TX	$g_o$	small-signal material gain coefficient of the SOA
$z_n$	coordinate of the end of the $n^{\text{th}}$ span [m]	$g_o$	small-signal integrated gain coefficient of the SOA
$\Delta L$	span length [m]	$g_n(z, t)$	small-signal material gain of the $n^{\text{th}}$ SOA [1/m]
$L$	total transmission distance [m]	$g_n(t)$	integrated gain coefficient of the $n^{\text{th}}$ SOA
$N_s$	number of spans	$\mathcal{I}_k$	$k^{\text{th}}$ sample of matched filtered photocurrent
COI	channel of interest	$b_k$	nonlinear signal-signal distortion of the $k^{\text{th}}$ received symbol
$s$	WDM channels discrete index	$n_k$	ASE noise samples of the $k^{\text{th}}$ received symbol of COI
$M$	number of WDM channels on each side of the COI	$u_f(t)$	impulse response of the matched filter
$\Delta\Omega$	channel spacing [rad./s]	$E(z, t)$	optical field [ $\sqrt{W}$ ]
$\Omega_s$	base-band center frequency of the $s^{\text{th}}$ WDM channel	$A_0(z, t)$	pulse-shape at TX [ $\sqrt{W}$ ]
$\delta T_s$	time shift between COI and the $s^{\text{th}}$ channel at TX	$U(z, t)$	power normalized optical field [ $\sqrt{W}$ ]
$\phi_s(0)$	time shift between COI and the $s^{\text{th}}$ channel at TX	$U_0(z, t)$	power normalized pulse-shape at TX [ $\sqrt{W}$ ]
$\mathcal{E}$	pulse energy [J]	$n(z, z, t)$	ASE noise process [ $\sqrt{W}$ ]
$P$	channel average power [W]	$\dagger$	Hermitian conjugation
$T$	symbol duration [s]	$*$	complex conjugation
$k, m, n, p$	various discrete indices	$\langle \rangle$	time and/or ensemble average
$a_k$	$k^{\text{th}}$ information symbol of the COI	$\langle \cdot \rangle$	time and/or frequency cross-correlation operator. cf. App.A
$a_{k,s}$	$k^{\text{th}}$ information symbol of the $s^{\text{th}}$ WDM channel	$\delta(\cdot)$	Dirac delta function
$\mu_n$	$n^{\text{th}}$ moment of the constellation	$\theta(\cdot)$	Heaviside unit step function
$S_n$	signal power launched into the $n^{\text{th}}$ span	$\delta_{mn}$	Kronecker delta function
$N_n$	output noise power generated by the $n^{\text{th}}$ SOA	$\mathcal{D}_z$	dispersion operator corresponding to a $z$ meter fiber. cf. App. A

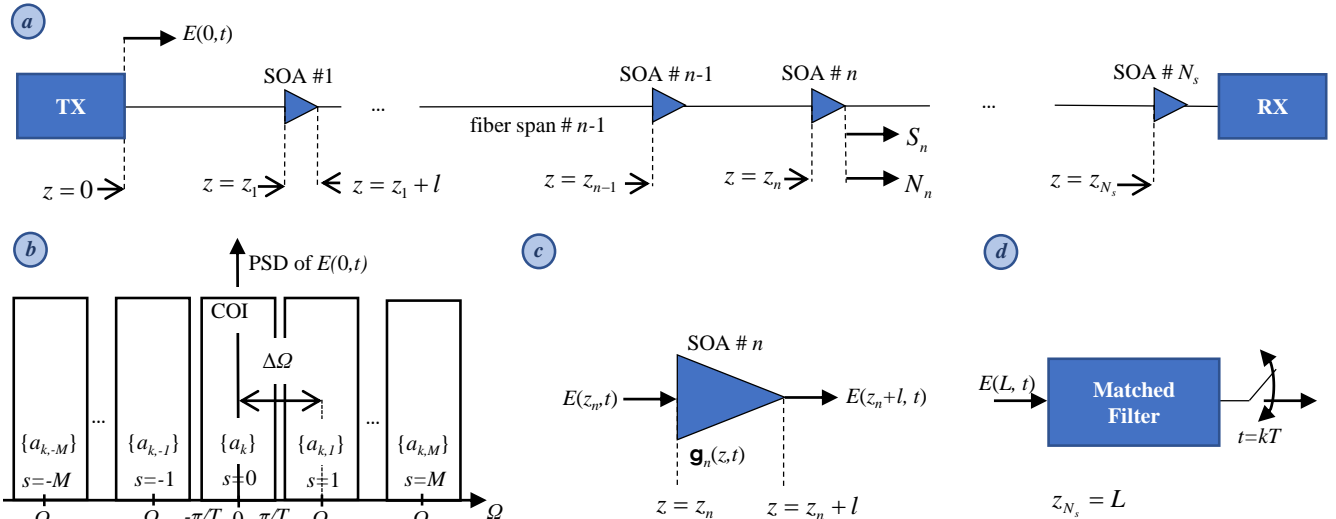


Fig. 1. (a): The fiber-optic multi-span link setup, composed of  $N_s$  spans. The  $n^{\text{th}}$  noisy SOA is placed at the end of the  $n^{\text{th}}$  span, i.e., at  $z = z_n$ . The transmitter, TX, is at  $z = z_0 = 0$ , and the receiver, RX, is at  $z = z_{N_s}$ . The total signal (noise) power at the output of the  $n^{\text{th}}$  SOA is  $S_n$  ( $N_n$ ). (b): the power spectral density (PSD) of the total optical field  $E(0, t)$  at TX output, COI: channel of interest,  $a_{k,s}$  is the  $k^{\text{th}}$  information of symbol of the  $s^{\text{th}}$  channel,  $s = 0$  corresponds to COI.  $a_k$  is the  $k^{\text{th}}$  information of symbol of the COI. (c): the  $n^{\text{th}}$  SOA placed at the end of the  $n^{\text{th}}$  span, i.e.,  $z = z_n$ . The SOA cavity length is  $l$ . The material gain of the  $n^{\text{th}}$  SOA is  $g_n(z, t)$  inside the SOA cavity. (d): the ideal coherent RX to receive the COI, composed of the matched filter followed by symbol-spaced sampler.

We define the integrated gain coefficient of the  $n^{\text{th}}$  amplifier,  $g_n(t)$  as follows

$$g_n(t) = \int_{z_n}^{z_n+l} dz g_n(z, t). \quad (6)$$

Similarly, the integrated small-signal gain of the  $n^{\text{th}}$  SOA is defined as  $g_o = g_o l$ . It is a well-known fact that the  $z$  dependence in (3) and (5) can be integrated out, to find the following input-output equations for modeling the  $n^{\text{th}}$  SOA

$$\tau_c \frac{d}{dt} g_n(t) = g_o - g_n(t) - \epsilon \left[ e^{g_n(t)} - 1 \right] |E(z_n, t)|^2, \quad (7)$$

and

$$E(z_n + l, t) = \exp \left\{ \frac{1}{2} (1 - i\alpha_H) g_n(t) \right\} E(z_n, t). \quad (8)$$

### C. System model

Signal propagation in each fiber span is modeled by the nonlinear Schrödinger equation (NLSE) [5]

$$\partial_z E(z, t) = -\frac{\alpha}{2} E(z, t) - i\frac{\beta_2}{2} \partial_t^2 E(z, t) + i\gamma |E(z, t)|^2 E(z, t). \quad (9)$$

Note that (9) is valid for

$$z_{n-1} + l \leq z \leq z_n, \text{ for } n = 1, \dots, N_s. \quad (10)$$

On the other hand, for  $z_n \leq z \leq z_n + l$ , the propagation of the optical field inside SOA waveguides is modeled by (5). In fact, the multi-span link is a cascade of  $N_s$  nonlinear fiber spans described by the NLSE interleaved with  $N_s$  nonlinear SOAs modeled by (7) and (8).

Next, we derive a single partial differential equation describing the field propagation in the whole multi-span link. Note that the SOA waveguide cavity length,  $l$ , is on the order of millimeters, whereas the span length is a few tens of kilometer; therefore, we let  $l \rightarrow 0$ , and  $g_o \rightarrow \infty$ , but such that the product  $g_o l$  remains constant and equal to  $g_o$ . Moreover, we assume that the material gain coefficient of the SOA is a constant function of  $z$  inside the SOA waveguide, and is written as

$$\mathbf{g}_n(z, t) = g_n(t) p_l(z - z_n), \quad (11)$$

where,

$$p_l(z) = \begin{cases} 1/l & 0 \leq z \leq l \\ 0 & \text{otherwise} \end{cases}. \quad (12)$$

Note that when the SOA cavity length tends to zero, we have  $\lim_{l \rightarrow 0} p_l(z) = \delta(z)$ , where  $\delta(\cdot)$  is the Dirac delta function. So, in the  $l \rightarrow 0$  limit we have

$$\lim_{l \rightarrow 0} \mathbf{g}_n(z, t) = g_n(t) \delta(z - z_n). \quad (13)$$

Now, we define the following overall material gain coefficient function across the whole link from  $z = 0$  to  $z = z_{N_s}$ .

$$\mathbf{g}(z, t) = \sum_{n=1}^{N_s} g_n(t) \delta(z - z_n). \quad (14)$$

Using (14), we can describe the field propagation from  $z = 0$  to  $z = z_{N_s}$  by a single partial differential equation, which is

$$\begin{aligned} \partial_z E(z, t) &= \frac{1}{2} (1 - i\alpha_H) \mathbf{g}(z, t) E(z, t) \\ &- \frac{\alpha}{2} E(z, t) - i\frac{\beta_2}{2} \partial_t^2 E(z, t) + i\gamma |E(z, t)|^2 E(z, t) + n(z, t). \end{aligned} \quad (15)$$

In (15), we have manually added the spatio-temporal ASE process  $n(z, t)$ . It is a circular complex Gaussian process with zero mean and the following spectral domain autocorrelation

$$\langle \tilde{n}^*(z, \omega) \tilde{n}(z', \omega') \rangle = 2\pi \tilde{C}(z, \omega) \delta(z - z') \delta(\omega - \omega'). \quad (16)$$

where, we have

$$\tilde{C}(z, \omega) = \frac{\hbar\omega_0}{2} n_{\text{sp}} \sum_{n=1}^{N_s} (e^{\bar{g}_n} - 1) \delta(z - z_n). \quad (17)$$

Note that although the field propagation is described by a single equation, (15), we still have  $N_s$  reservoir equations for the gain dynamics of the SOAs, (cf. (7), and note that  $n = 1, \dots, N_s$ ), coupled to the propagation equation (15). Our next task is to analyze the SOAs' nonlinear gain fluctuations in term of perturbation series in  $\epsilon$ , and derive a single propagation equation that includes the gain dynamics of all the amplifiers as well.

### D. Perturbation analysis of gain dynamics

Let's write the integrated gain coefficient of the  $n^{\text{th}}$  SOA as

$$g_n(t) = \bar{g}_n + \delta g_n(t), \quad (18)$$

where,  $\bar{g}_n$  is the time averaged integrated gain coefficient, *i.e.*,

$$\bar{g}_n = \langle g_n(t) \rangle, \quad (19)$$

and  $\delta g_n(t)$  is the zero-mean integrated gain fluctuations. In order to obtain the equation governing  $g_n$ , we compute the time average of both sides of (7). We obtain

$$0 = g_o - \bar{g}_n - \epsilon \left\langle \left( e^{\bar{g}_n} e^{\delta g_n(t)} - 1 \right) |E(z_n, t)|^2 \right\rangle. \quad (20)$$

We keep only first-order fluctuations of gains and optical field intensity in the analysis. Based on this approximation we have

$$e^{\delta g_n(t)} \cong 1 + \delta g_n(t). \quad (21)$$

We also assume the second-order fluctuations  $\langle \delta g_n(t) \delta |E(z_n, t)|^2 \rangle$  are negligible, thus

$$\langle \delta g_n(t) |E(z_n, t)|^2 \rangle = \langle \delta g_n(t) \rangle \langle |E(z_n, t)|^2 \rangle = 0. \quad (22)$$

Using (21) and (22), we find the following equation for the average gain of the  $n^{\text{th}}$  SOA

$$0 = g_o - \bar{g}_n - \epsilon (e^{\bar{g}_n} - 1) \langle |E(z_n, t)|^2 \rangle. \quad (23)$$

We neglect signal depletion by ASE noise, and assume that average gain perfectly compensates the span loss. In other words,

$$\bar{g}_n = \alpha \Delta L. \quad (24)$$

Let's denote the power span loss by  $\eta$ , which is

$$\eta = e^{-\alpha \Delta L}. \quad (25)$$

Note that

$$\langle |E(z_n, t)|^2 \rangle = \eta P_{\text{tot}}. \quad (26)$$

The  $P_{\text{tot}}$  is the total power at the output of each SOA. We have  $P_{\text{tot}} = N_{\text{ch}} P$ , where  $N_{\text{ch}}$  is the number of WDM channels. In this work, we assume  $N_{\text{ch}}$  is an odd number,  $N_{\text{ch}} = 2M + 1$ , and that the COI is the  $(M + 1)^{\text{th}}$  channel located at the center of the WDM grid (cf. Fig. 1.b). Using (21)-(26), the (20) results in

$$\alpha \Delta L + \epsilon (1 - \eta) P_{\text{tot}} = g_o. \quad (27)$$

Now, using (7), (18), (23), and (27), we find the following equation for the gain fluctuations

$$\tau_c \frac{d}{dt} \delta g_n(t) + \delta g_n(t) = \epsilon(1 - \eta) P_{tot} - \epsilon e^{\bar{g}_n} \delta g_n(t) |E(z_n, t)|^2 - \epsilon(e^{\bar{g}_n} - 1) |E(z_n, t)|^2. \quad (28)$$

Now we expand the integrated gain coefficient zero-mean fluctuations and the electrical field in terms of regular perturbation series with respect to the parameter  $\epsilon$ , as

$$\delta g_n(t) = \sum_{m=0}^{\infty} \epsilon^m \delta g_n^{(m)}(t), \quad (29)$$

and

$$E(z, t) = \sum_{m=0}^{\infty} \epsilon^m E^{(m)}(z, t). \quad (30)$$

In (29) and (30)  $\delta g_n^{(m)}$ , and  $E^{(m)}$ , are the  $m^{\text{th}}$  order perturbation corrections to the integrated gain coefficient and the optical field respectively. In the sequel we will only compute terms up to the first order in  $\epsilon$ . The FRP approximations to the integrated gain and the optical field are

$$\delta g_{n,FRP}(t) = \delta g_n^{(0)}(t) + \epsilon \delta g_n^{(1)}(t), \quad (31)$$

and

$$E_{FRP}(z, t) = E^{(0)}(z, t) + \epsilon E^{(1)}(z, t). \quad (32)$$

Note that

$$\delta g_n(t) = \delta g_{n,FRP}(t) + \mathcal{O}(\epsilon^2), \quad (33)$$

and

$$E(z, t) = E_{FRP}(z, t) + \mathcal{O}(\epsilon^2). \quad (34)$$

Now we substitute (29), and (30) into (28), and extract the equations for zeroth and first order perturbations. The equation governing the zeroth-order integrated gain fluctuations is

$$\tau_c \frac{d}{dt} \delta g_n^{(0)}(t) + \delta g_n^{(0)}(t) = 0. \quad (35)$$

Similarly, we derive the following equation for the first-order perturbation correction to the integrated gain coefficient

$$\tau_c \frac{d}{dt} \delta g_n^{(1)}(t) + \delta g_n^{(1)}(t) = (1 - \eta) P_{tot} - e^{\bar{g}_n} \delta g_n^{(0)}(t) |E^{(0)}(z_n, t)|^2 - (e^{\bar{g}_n} - 1) |E^{(0)}(z_n, t)|^2. \quad (36)$$

We suppose that the system is turned on in  $t = -\infty$ , and that transient solutions of (35) and (36) are tended to zero. Based on this assumption we have

$$\delta g_n^{(0)}(t) = 0. \quad (37)$$

Now we substitute (37) into (36), and solve (36) to obtain

$$\delta g_n^{(1)}(t) = (1 - \eta) P_{tot} - (e^{\bar{g}_n} - 1) \int_{-\infty}^{+\infty} d\tau r_c(\tau) |E^{(0)}(z_n, t - \tau)|^2. \quad (38)$$

The  $r_c(\cdot)$  is the carrier density pulsation (CDP) impulse response of the  $n^{\text{th}}$  SOA carrier reservoir. It is explicitly written as

$$r_c(t) = \frac{1}{\tau_c} e^{-t/\tau_c} \theta(t). \quad (39)$$

The function  $\theta(\cdot)$  is the Heaviside unit step function. Note that  $\int_{-\infty}^{+\infty} r_c(t) dt = 1$ ; therefore, as a sanity check, we calculate  $\langle \delta g_n^{(1)}(t) \rangle = 0$ .

We substitute (18), into (14), and derive the following expression for the FRP approximation of the overall material gain coefficient

$$\mathbf{g}_{FRP}(z, t) = \mathbf{g}^{(0)}(z) + \epsilon \mathbf{g}^{(1)}(z, t), \quad (40)$$

where,

$$\mathbf{g}^{(0)}(z) = \sum_{n=1}^{N_s} \bar{g}_n \delta(z - z_n). \quad (41)$$

$$\mathbf{g}^{(1)}(z, t) = -d(z) \int_{-\infty}^{+\infty} d\tau r_c(\tau) |E^{(0)}(z, t - \tau)|^2, \quad (42)$$

where

$$d(z) = (e^{\bar{g}_n} - 1) \sum_{n=1}^{N_s} \delta(z - z_n). \quad (43)$$

In writing (42) we used the *sifting* property of Dirac delta function, *i.e.*,

$$|E^{(0)}(z_n, t)|^2 \delta(z - z_n) = |E^{(0)}(z, t)|^2 \delta(z - z_n). \quad (44)$$

From now on, we work with  $\mathbf{g}_{FRP}$  instead of  $\mathbf{g}$ . We substitute (40) into (15), and obtain an FRP approximation to the NLSE (FNLSE), which is

$$\begin{aligned} \partial_z E(z, t) &= \frac{1}{2} (1 - i\alpha_H) \mathbf{g}^{(0)}(z) E(z, t) \\ &+ \epsilon \frac{1}{2} (1 - i\alpha_H) \mathbf{g}^{(1)}(z, t) E(z, t) \\ &- \frac{\alpha}{2} E(z, t) - i \frac{\beta_2}{2} \partial_t^2 E(z, t) + i\gamma |E(z, t)|^2 E(z, t) \end{aligned} \quad (45)$$

At this point, we define the power normalized optical field  $U(z, t)$  by the following equation

$$E(z, t) = \sqrt{\mathcal{E}} \exp \left\{ \frac{1}{2} (1 - i\alpha_H) \int_0^z dz' \mathbf{g}^{(0)}(z') - \frac{\alpha z}{2} \right\} U(z, t). \quad (46)$$

The Perturbation series of the normalized field is

$$U(z, t) = \sum_{m=0}^{\infty} \epsilon^m U^{(m)}(z, t). \quad (47)$$

The noormalization relation, (46), is extended to all orders of perturbation  $m = 0, \dots, \infty$ , *i.e.*,

$$\begin{aligned} E^{(m)}(z, t) &= \sqrt{\mathcal{E}} \exp \left\{ \frac{1}{2} (1 - i\alpha_H) \int_0^z dz' \mathbf{g}^{(0)}(z') - \frac{\alpha z}{2} \right\} U^{(m)}(z, t). \end{aligned} \quad (48)$$

After substituting (46) into (45) and simplification, we obtain the following normalized FNLSE

$$\begin{aligned} \partial_z U(z, t) = & -i \frac{\beta_2}{2} \partial_t^2 U(z, t) + i \gamma \mathcal{E} f(z) |U(z, t)|^2 U(z, t) \\ & - \epsilon \mathcal{E} \frac{1}{2} (1 - i \alpha_H) \mathbf{d}(z) f(z) \times \\ & \int_{-\infty}^{+\infty} d\tau r_c(\tau) |U^{(0)}(z, t - \tau)|^2 U(z, t) + \frac{n(z, t)}{\sqrt{\mathcal{E} f(z)}}. \end{aligned} \quad (49)$$

The function  $f(z)$  is

$$f(z) = e^{-\alpha(z - z_{n-1})}, \quad z_{n-1} \leq z \leq z_n, n = 1, \dots, N_s. \quad (50)$$

Equation (49) is the main result of this section. We can describe the whole system by a single equation at the cost of treating the SOA gain fluctuations as first order perturbations in terms of the reciprocal of SOA saturation power, denoted by  $\epsilon$ . The first and second terms on the right hand side of (49) correspond to the fiber group velocity dispersion (GVD) and fiber Kerr nonlinearity. If the amplifiers are linear,  $\epsilon = 0$ , and  $g_n(t) = \alpha \Delta L$ ; otherwise, the third term models the nonlinear distortions induced by the cascade of the SOAs as the optical field propagates along the multi-span link. In the next section, we present the FRP analysis of the normalized FNLSE, (49), in terms of both  $\epsilon$  and  $\gamma$ .

### E. Perturbation analysis of the normalized FNLSE

We substitute the perturbation series of the power normalized optical field,  $U(z, t)$ , in terms of the SOA nonlinear parameter  $\epsilon$ , *i.e.*, equation (47) into (49). The equation for the zeroth order term,  $U^{(0)}(z, t)$ , is

$$\begin{aligned} \partial_z U^{(0)}(z, t) = \\ -i \frac{\beta_2}{2} \partial_t^2 U^{(0)}(z, t) + i \gamma \mathcal{E} f(z) |U^{(0)}(z, t)|^2 U^{(0)}(z, t). \end{aligned} \quad (51)$$

We consider the perturbation series of  $U^{(0)}(z, t)$  in terms of the fiber nonlinear coefficient  $\gamma$

$$U^{(0)}(z, t) = u^{(0,0)}(z, t) + \gamma u^{(0,1)}(z, t) + \mathcal{O}(\gamma^2). \quad (52)$$

We substitute (52) into (51) and obtain the following equations for the zeroth-order and first-order perturbation series (with respect to  $\gamma$ ) terms of  $U^{(0)}$ . For the zeroth-order term we have

$$\partial_z u^{(0,0)}(z, t) = -i \frac{\beta_2}{2} \partial_t^2 u^{(0,0)}(z, t) + \frac{n(z, t)}{\sqrt{\mathcal{E} f(z)}}, \quad (53)$$

and, for the first-order term we have

$$\begin{aligned} \partial_z u^{(0,1)}(z, t) = \\ -i \frac{\beta_2}{2} \partial_t^2 u^{(0,1)}(z, t) + i \gamma \mathcal{E} f(z) |u^{(0,0)}(z, t)|^2 u^{(0,0)}(z, t). \end{aligned} \quad (54)$$

In this work, we ignore all the second-order perturbation terms, *i.e.*, the terms of the order of  $\mathcal{O}(\epsilon^2)$ ,  $\mathcal{O}(\gamma^2)$ , and  $\mathcal{O}(\epsilon\gamma)$ .

Adopting this approximation, the equation for the first-order perturbation terms with respect to  $\epsilon$  is

$$\begin{aligned} \partial_z U^{(1)}(z, t) = \\ -i \frac{\beta_2}{2} \partial_t^2 U^{(1)}(z, t) - \epsilon \mathcal{E} \frac{1}{2} (1 - i \alpha_H) f(z) \mathbf{d}(z) \times \\ \int_{-\infty}^{+\infty} d\tau r_c(\tau) |u^{(0,0)}(z, t - \tau)|^2 u^{(0,0)}(z, t). \end{aligned} \quad (55)$$

### F. Solutions of the zeroth-order and first-order equations

The solution of (53) is

$$\begin{aligned} u^{(0,0)}(z, t) = \sum_k a_k u_k^{(0,0)}(z, t) + \\ \sum_{k,s \neq 0} a_{k,s} u_{k,s}^{(0,0)}(z, t - t_s(z)) \exp[-i \Omega_s t + i \phi_s(z)] + \\ \hat{\mathcal{D}}_z [u_{\text{ASE}}(z, t)], \end{aligned} \quad (56)$$

where<sup>2</sup>

$$u_{\text{ASE}}(z, t) = \int_0^z dz' \frac{n(z', t)}{\sqrt{\mathcal{E} f(z')}}. \quad (57)$$

The zeroth-order dispersed pulse of the  $k^{\text{th}}$  symbol of the  $s^{\text{th}}$  channel after propagating up to distance  $z$  is

$$u_{k,s}^{(0,0)}(z, t) = \hat{\mathcal{D}}_z [u_{k,s}^{(0,0)}(0, t)]. \quad (58)$$

The same expression holds for COI, albeit with dropping the subscript  $s$ . The  $u_0^{(0,0)}(0, t)$  is the unperturbed pulse-shape of the COI, which is

$$u_0^{(0,0)}(0, t) = \frac{1}{\sqrt{T}} \text{sinc} \left( \frac{t}{T} \right). \quad (59)$$

All the adjacent channels use the same pulse-shape as the COI. The time shift between COI and the  $s^{\text{th}}$  channel, after propagation up to distance  $z$  is

$$t_s(z) = \delta T_s + \beta_2 \Omega_s z. \quad (60)$$

The relative phase shift between COI and the  $s^{\text{th}}$  channel, after propagation up to distance  $z$  is

$$\phi_s(z) = \phi_s(0) + \frac{\beta_2 \Omega_s^2 z}{2}. \quad (61)$$

We suppose  $\delta T_s = 0$ ,  $\phi_s(0) = 0$ , and  $\Omega_s = s \Delta \Omega$ , in the rest of the work.

The solution of (54) is presented in Eq. (90) of [7] (cf. also [14] and [15]), and will not be repeated here. The solution of (55) is

$$\begin{aligned} U^{(1)}(z, t) = \epsilon \mathcal{E} \frac{1}{2} (1 - i \alpha_H) \hat{\mathcal{D}}_z \int_0^z dz' \mathbf{d}(z') f(z') \times \\ \hat{\mathcal{D}}_z^\dagger \left[ \int_{-\infty}^{+\infty} d\tau r_c(\tau) |u^{(0,0)}(z', t - \tau)|^2 u^{(0,0)}(z', t) \right]. \end{aligned} \quad (62)$$

<sup>2</sup>cf. [14] and the discussion leading to Eq. (72) in [7].

### G. Sampled photocurrent analysis

The ideal coherent receiver in this work consists of a matched filter to the COI pulse-shape followed by ideal symbol-spaced sampling. cf. Fig. 1.c. The impulse response of the matched filter,  $u_f$ , is given by

$$u_f^*(-t) = \hat{D}_L \left[ u_0^{(0,0)}(0, t) \right], \quad (63)$$

The sampled photocurrent  $\mathcal{I}_k$  is given by the following equation

$$\mathcal{I}_k = \left\langle \hat{D}_L \left[ u_k^{(0,0)}(0, t) \right], U(L, t) \right\rangle. \quad (64)$$

The FRP approximation to  $\mathcal{I}_k$  is denoted by  $\mathcal{J}_k$ . We have

$$\mathcal{I}_k = \mathcal{J}_k + \mathcal{O}(\epsilon^2) + \mathcal{O}(\gamma^2) + \mathcal{O}(\epsilon\gamma). \quad (65)$$

From now on, we study only the  $\mathcal{J}_k$ . It is given by

$$\mathcal{J}_k = \left\langle \hat{D}_L \left[ u_k^{(0,0)}(0, t) \right], U_{FRP}(L, t) \right\rangle, \quad (66)$$

where

$$U_{FRP}(z, t) = u^{(0,0)}(z, t) + \gamma u^{(0,1)}(z, t) + \epsilon U^{(1)}(z, t). \quad (67)$$

We substitute (67) into (66), and we obtain

$$\mathcal{J}_k = a_k + b_k + b'_k + n_k, \quad (68)$$

where  $a_k$  is the  $k^{\text{th}}$  symbol of the COI,  $b_k$  is the total fiber-induced SS nonlinear distortion, and  $b'_k$  is the total SOA-induced SS nonlinear distortions. The detailed analysis of  $b_k$ , using exactly the same notation as this work, is presented in [7] (cf. also [14] and [15]). Here, we focus on the SOA-induced nonlinear distortions. We have

$$b'_k = \left\langle \hat{D}_L \left[ u_k^{(0,0)}(0, t) \right], U^{(1)}(L, t) \right\rangle. \quad (69)$$

Now we substitute (62) into (69) and use the dispersion exchange formula (81), [7], [14]. We obtain

$$b'_k = \epsilon \mathcal{E} \frac{1}{2} (1 - i\alpha_H) \int_0^L dz d(z) f(z) \int_{-\infty}^{+\infty} dt u_k^{(0,0)}(z, t) \times \int_{-\infty}^{+\infty} d\tau r_c(\tau) |u^{(0,0)}(z, t - \tau)|^2 u^{(0,0)}(z, t). \quad (70)$$

### H. Computing the variance of nonlinear distortions

In this section we give the expressions for the variance of the terms on the right hand side of (68). The variance of the ASE,  $\sigma_{ASE}^2 = \langle |n_k|^2 \rangle$  is (cf. Eq. (98) in [7])

$$\sigma_{ASE}^2(P) = \frac{\hbar\omega_0}{2PT} n_{sp} (e^{\bar{g}} - 1) N_s. \quad (71)$$

The variance of single polarization signal-signal fiber-induced total nonlinear distortions,  $\sigma_{SS,f}^2 = \langle |b_k|^2 \rangle$ , is given by (cf. Eq. (105) in [7])

$$\begin{aligned} \sigma_{SS,f}^2(P) = & \gamma^2 P^2 \{ 2\mathcal{X}_1 + \left(\frac{\mu_4}{\mu_2} - 2\right) [\mathcal{X}_2 + 4\mathcal{X}_3 + 4\mathcal{X}_4] + \\ & \left(\frac{\mu_6}{\mu_2} - 9\frac{\mu_4}{\mu_2} + 12\right) \mathcal{X}_5 + 4 \sum_s [\mathcal{X}_{1,s} + \left(\frac{\mu_4}{\mu_2} - 2\right) \mathcal{X}_{3,s}] + \\ & \sum_s \sum_{s'} \mathcal{X}_{1,s,s'} \}, \quad (72) \end{aligned}$$

where the  $\mu_n$  is the  $n^{\text{th}}$  moment of the constellations, and the various  $\mathcal{X}$  coefficients on the right hand side of (72) are given by Eqs. (202)-(208) in [7].

The new contribution of this work, is calculating the variance of signal-signal SOA-induced total nonlinear distortions  $\sigma_{SS,s}^2 = \langle |b'_k|^2 \rangle$ . It is given by

$$\begin{aligned} \sigma_{SS,s}^2(P) = & \frac{1}{4} \epsilon^2 P^2 (1 + \alpha_H^2) (\bar{G} - 1)^2 \{ 2\mathcal{Y}_1 + \left(\frac{\mu_4}{\mu_2} - 2\right) [\mathcal{Y}_2 + 4\mathcal{Y}_3 + 4\mathcal{Y}_4] + \\ & \left(\frac{\mu_6}{\mu_2} - 9\frac{\mu_4}{\mu_2} + 12\right) \mathcal{Y}_5 + 4 \sum_s [\mathcal{Y}_{1,s} + \left(\frac{\mu_4}{\mu_2} - 2\right) \mathcal{Y}_{3,s}] + \\ & \sum_s \sum_{s'} \mathcal{Y}_{1,s,s'} \}, \quad (73) \end{aligned}$$

where  $\bar{G} = e^{\bar{g}}$ , and the  $\mathcal{Y}$  coefficients on the right hand side of (73) are computed in the Appendix. B.

## III. CONCLUSIONS

We presented for the first time, a theory of signal propagation in multi-span wavelength division multiplexed coherent transmission systems, which use in-line semiconductor optical amplifiers (SOA). The SOAs were modeled by a standard reservoir model. The reciprocal of the SOA saturation power was treated as a new second perturbation parameter, besides the fiber nonlinear coefficient. First, an equivalent nonlinear Schrödinger equation, capturing both signal propagation in fiber and the SOAs gain dynamics was derived. Then time-domain first-order regular perturbation theory was applied to this equation, and the signal-to-noise ratio of the sampled received photocurrent was computed.

## APPENDIX

### A. Notations and preliminary material

The Fourier transform pair in this work is

$$\tilde{x}(z, \omega) = \mathcal{F}[x(z, t)] = \int_{-\infty}^{+\infty} dt \exp(i\omega t) x(z, t), \quad (74)$$

$$x(z, t) = \mathcal{F}^{-1}[\tilde{x}(z, \omega)] = \frac{1}{2\pi} \int_{-\infty}^{+\infty} d\omega \exp(-i\omega t) \tilde{x}(z, \omega), \quad (75)$$

where,  $\mathcal{F}$  stands for the Fourier transform,  $\mathcal{F}^{-1}$  stands for the inverse Fourier transform,  $\omega = 2\pi f$  is the angular frequency, and  $f$  is the frequency. Throughout this paper, a waveform with a tilde on top is the Fourier transform of the waveform denoted by the same symbol but without tilde. We define the following notations for waveforms cross-correlations in time domain

$$\langle x(z, t), y(z', t') \rangle = \int_{-\infty}^{+\infty} d\tau x^*(z, t + \tau) y(z', t' + \tau), \quad (76)$$

and in frequency domain

$$\langle \tilde{x}(z, \omega), \tilde{y}(z', \omega') \rangle = \int_{-\infty}^{+\infty} d\nu \tilde{x}^*(z, \omega + \nu) \tilde{y}(z', \omega' + \nu), \quad (77)$$

where, the superscript  $*$  stands for complex conjugation. On the other hand, we use the notation  $\langle x(z, t) \rangle$  to denote the ensemble average over the space of all sample waveforms of the stochastic process  $x(z, t)$ . The randomness of the processes in this work is due to information symbols, which are assumed to be independent identically distributed (i.i.d.) discrete random variables with phase-isotropic distributions, and also due to amplifier noise. In our notation, the Parseval's theorem is stated as follows

$$\langle x(z, t), y(z', t) \rangle = \frac{1}{2\pi} \langle \tilde{x}(z, \omega), \tilde{y}(z', \omega) \rangle. \quad (78)$$

We introduce the following notation for the dispersion operator in the frequency domain

$$\hat{D}_{z'} [\tilde{x}(z, \omega)] = \exp\left(i\frac{\omega^2}{2} \int_0^{z'} dz'' \beta_2(z'')\right) \tilde{x}(z, \omega), \quad (79)$$

and in the time domain

$$\hat{D}_{z'} [x(z, t)] = \mathcal{F}^{-1} \left[ \exp\left(i\frac{\omega^2}{2} \int_0^{z'} dz'' \beta_2(z'')\right) \tilde{x}(z, \omega) \right]. \quad (80)$$

The following *dispersion exchange formula* (DEF), which is easily proven by Parseval's theorem, will be extensively used in this work (cf. Eqs.(19) and (20) in [14])

$$\langle x(z, t), \hat{D}_{z'} [y(z, t)] \rangle = \langle \hat{D}_{z'}^\dagger [x(z, t)], y(z, t) \rangle, \quad (81)$$

where,  $\hat{D}_{z'}^\dagger$  is the adjoint of the dispersion operator  $\hat{D}_{z'}$ , which is defined to be

$$\hat{D}_{z'}^\dagger [\tilde{x}(z, \omega)] = \exp\left(-i\frac{\omega^2}{2} \int_0^{z'} dz'' \beta_2(z'')\right) \tilde{x}(z, \omega). \quad (82)$$

Finally note that the sinc function is

$$\text{sinc}(x) = \frac{\sin(\pi x)}{\pi x}. \quad (83)$$

### B. Computing the noise variance of SOA-induced nonlinearity

In this section we outline the computation of the variance of signal-signal SOA-induced nonlinear distortions  $\sigma_{SS,s}^2$ . We substitute the signal terms on right hand side of (56) into (70). We ignore nonlinear noise-signals interaction in the SOA in this work. The resulting expression is

$$\begin{aligned} b'_k &= \sum_{m,n,p} a_{m+k} a_{n+k} a_{p+k}^* Y_{m,n,p}^{(0,0)} + \\ & 2 \sum_s \sum_{m,n,p} a_{m+k} a_{n+k,s} a_{p+k,s}^* Y_{m,n,p}^{(0,s)} + \\ & \sum_{\substack{s,s' \\ s \neq s'}} \sum_{m,n,p} a_{m+k,s} a_{n+k,s'} a_{p+k,s+s'}^* Y_{m,n,p}^{(s,s')}, \end{aligned} \quad (84)$$

where,

$$\begin{aligned} Y_{m,n,p}^{(s,s')} &= \int_{-\infty}^{+\infty} \int_{-\infty}^{+\infty} dt d\tau r_c(\tau) u_0^{(0,0)*}(z, t) \times \\ & u_m^{(0,0)}(z, t - t_s - \tau) u_n^{(0,0)}(z, t - t_{s'}) \times \\ & u_p^{(0,0)*}(z, t - t_{s+s'} - \tau). \end{aligned} \quad (85)$$

these coefficients are expressed in the spectral domain as follows

$$Y_{m,n,p}^{(s,s')} = \int_{\mathbb{R}^3} \frac{d^3\omega}{(2\pi)^3} H'_{\vec{\omega},s,s'}(z) e^{i(m\omega_1 - p\omega_2 + n\omega_3)T}. \quad (86)$$

The symbol  $d^n\omega$  stands for  $d\omega_1 d\omega_2 \cdots d\omega_n$  for any positive integer  $n$ , and the following notational convention is used

$$\vec{\omega} = (\omega_1, \omega_2, \omega_3). \quad (87)$$

The integrand function is

$$\begin{aligned} H'_{\vec{\omega},s,s'}(z) &= \Pi_{\vec{\omega},s,s'} d(z) f(z) \times \\ & e^{i\beta_2 z[(\omega_2 - \omega_3)(\omega_2 - \omega_1) - s s' \Delta \Omega^2]}. \end{aligned} \quad (88)$$

The function  $\Pi'_{\vec{\omega},s,s'}$  is defined to be

$$\begin{aligned} \Pi'_{\vec{\omega},s,s'} &= \tilde{r}_c(\omega_1 - \omega_2 - \Omega_{s'}) \tilde{u}_0^{(0)}(0, \omega_1 - \Omega_s) \times \\ & \tilde{u}_0^{(0)*}(0, \omega_2 - \Omega_{s+s'}) \tilde{u}_0^{(0)}(0, \omega_3 - \Omega_{s'}) \tilde{u}_0^{(0)*}(0, \omega_1 - \omega_2 + \omega_3). \end{aligned} \quad (89)$$

The following notional simplifications are used:  $H'_{\vec{\omega},s} = H'_{\vec{\omega},0,s}$ ,  $\Pi'_{\vec{\omega},s} = \Pi'_{\vec{\omega},0,s}$ ,  $H'_{\vec{\omega}} = H'_{\vec{\omega},0,0}$ , and  $\Pi'_{\vec{\omega}} = \Pi'_{\vec{\omega},0,0}$ <sup>3</sup>.

The rest of derivation follows exactly the steps detailed in the Appendix of [7] for the derivation of  $\mathcal{X}$  coefficients. In order to define  $\mathcal{Y}$  coefficients, take Eqs. (134)-(141) of [7], and replace  $X$ , and  $\mathcal{X}$  by  $Y$  and  $\mathcal{Y}$  respectively everywhere in those equations. The next step is writing the integral representations for the  $\mathcal{Y}$  coefficients, which are obtained by taking Eqs. (153)-(160) of [7], and replacing  $\mathcal{X}$  by  $\mathcal{Y}$  and  $H$  by  $H'$  everywhere in those equations. Finally, we use (43) and carry out  $z$ -integrations. The end results are

$$\mathcal{Y}_1 = \frac{1}{T} \int \frac{d^3\omega}{(2\pi)^3} \left| \sum_{m=1}^{N_s} r'_{\vec{\omega},m} \right|^2, \quad (90)$$

$$\mathcal{Y}_2 = \text{Re} \left\{ \int \frac{d^4\omega}{(2\pi)^4} \left( \sum_{m=1}^{N_s} r'_{\vec{\omega},m} \right) \left( \sum_{m=1}^{N_s} r'_{\vec{\omega}',m} \right) \right\}, \quad (91)$$

$$\mathcal{Y}_3 = \text{Re} \left\{ \int \frac{d^4\omega}{(2\pi)^4} \left( \sum_{m=1}^{N_s} r'_{\vec{\omega},m} \right) \left( \sum_{m=1}^{N_s} r'_{\vec{\omega}'',m} \right) \right\}, \quad (92)$$

$$\mathcal{Y}_5 = T \text{Re} \left\{ \int \frac{d^5\omega}{(2\pi)^5} \left( \sum_{m=1}^{N_s} r'_{\vec{\omega},m} \right) \left( \sum_{m=1}^{N_s} r'_{\vec{\omega}''',m} \right) \right\}, \quad (93)$$

$$\mathcal{Y}_{1,s} = \frac{1}{T} \int \frac{d^3\omega}{(2\pi)^3} \left| \sum_{m=1}^{N_s} r'_{\vec{\omega},m,s} \right|^2, \quad (94)$$

$$\mathcal{Y}_{3,s} = \text{Re} \left\{ \int \frac{d^4\omega}{(2\pi)^4} \left( \sum_{m=1}^{N_s} r'_{\vec{\omega},m,s} \right) \left( \sum_{m=1}^{N_s} r'_{\vec{\omega}'',m,s} \right) \right\}, \quad (95)$$

$$\mathcal{Y}_{1,s,s'} = \frac{1}{T} \int \frac{d^3\omega}{(2\pi)^3} \left| \sum_{m=1}^{N_s} r'_{\vec{\omega},m,s,s'} \right|^2, \quad (96)$$

<sup>3</sup>Note that the notations  $H_{\vec{\omega},s,s'}$ , and  $\Pi_{\vec{\omega},s,s'}$  are reserved for the treatment of the  $\mathcal{X}$  coefficients in [7]

The integrand function in is

$$r'_{\bar{\omega},m,s,s'} = \Pi'_{\bar{\omega},s,s'} e^{i\beta_2 z_m [(\omega_2 - \omega_3)(\omega_2 - \omega_1) - s s' \Delta \Omega^2]}. \quad (97)$$

Like for  $H'$ , and  $\Pi'$ , we adopt the following notational conventions:  $r'_{\bar{\omega},m,s} = r'_{\bar{\omega},m,0,s}$ ,  $r'_{\bar{\omega},m} = r'_{\bar{\omega},m,0,0}$ . The following shorthand notation are used in (90)-(96)

$$\bar{\omega}' = (\omega_4, \omega_2, \omega_1 + \omega_3 - \omega_4), \quad (98)$$

$$\bar{\omega}'' = (\omega_1, \omega_4, \omega_3 - \omega_2 + \omega_4), \quad (99)$$

and

$$\bar{\omega}''' = (\omega_4, \omega_5, \omega_1 - \omega_2 + \omega_3 - \omega_4 + \omega_5). \quad (100)$$

The  $\omega_i$ 's, for  $i = 1, \dots, 5$ , are independent real dummy integration variables.

## REFERENCES

- [1] A. Ghazisaeidi, I. Fernandez de Jauregui Ruiz, R. Rios-Mller, L. Schmalen, P. Tran, P. Brindel, A. Carbo Meseguer, Q. Hua, F. Buchali, G. Charlet, and J. Renaudier, "65Tb/s Transoceanic Transmission Using Probabilistically-Shaped PDM-64QAM," *in Proc. ECOC, Paper Th.3.C.4, Dsseldorf, Germany, 2016*.
- [2] A. Ghazisaeidi, I. Fernandez de Jauregui Ruiz, R. Rios-Mller, L. Schmalen, P. Tran, P. Brindel, A. Carbo Meseguer, Q. Hu, F. Buchali, G. Charlet and J. Renaudier, "Advanced C+L-Band Transoceanic Transmission Systems Based on Probabilistically-Shaped PDM-64QAM," *IEEE J. Lightwave Technol.*, vol. 35, no. 7, April 2017.
- [3] S. Zhang, F. Yaman, Y.-K. Huang, J. D. Downie, D. Zou, W. A. Wood, A. Zakharian, R. Khrapko, S. Mishra, V. Nazarov, J. Hurley, I. B. Djordjevic, E. Mateo, and Y. Inada., "Capacity-Approaching Transmission over 6375 km at Spectral Efficiency of 8.3 bit/s/Hz," *Proc. OFC, Th5C.2, Anaheim 2016*.
- [4] J.-X. Cai, H. Batshon, M. Mazurczyk, O. Sinkin, D. Wang, M. Paskov, C. Davidson, W. Patterson, M. Bolshtyansky, D. Foursa, "51.5 Tb/s Capacity over 17,107 km in C+L Bandwidth Using Single Mode Fibers and Nonlinearity Compensation," *in Proc. ECOC, paper Th.PDP. A2, Gotenborg, Sweden, 2017*.
- [5] G. P. Agrawal, "Nonlinear Fiber Optics," *Academic Press, 2007*.
- [6] R.-J. Essiambre, G. Kramer, P. J. Winzer, G. J. Foschini, B. Goebel, "Capacity Limits of Optical Fiber Networks," *IEEE J. Lightwave Technol.*, vol. 28, no. 4, February 2010.
- [7] A. Ghazisaeidi, "A Theory of Nonlinear Interactions between Signal and Amplified Spontaneous Emission Noise in Coherent Wavelength Division Multiplexed Systems," *J. Lightwave Technol., Early Access, DOI: 10.1109/JLT.2017.2764497, 2017*.
- [8] D. Qian, et al., "101.7-Tb/s PDM-128QAM-OFDM transmission over 3 55-km SSMF using pilot-based phase noise mitigation," *Proc. OFC, PDPB5, Los Angeles 2011*.
- [9] A. Sano et al., "102.3-Tb/s C-band extended L-band all-Raman transmission over 240 km using PDM-64QAM single carrier FDM with digital pilot tone," *Proc. OFC, PDPSC.3, Los Angeles 2012*.
- [10] M. J. Connelly, "Semiconductor optical amplifiers," *Springer Science and Business Media, 2007*.
- [11] T. Akiyama et al., "An Ultrawide-band (120 nm) Semiconductor Optical Amplifiers Having an Extremely-High Penalty-Free Output Power of 23 dBm Realized with Quantum-Dot Active Layers," *Proc. OFC, PDP12, 2004*.
- [12] J. Renaudier, A. Carbo Meseguer, A. Ghazisaeidi, P. Tran, R. Rios-Müller, R. Brenot, A. Verdier, F. Blache, K. Mekhazni, B. Duval, H. Debregeas, M. Achouche, A. Boutin, F. Morin, L. Letteron, N. Fontaine, Y. Frignac, G. Charlet, "First 100-nm Continuous-Band WDM Transmission System with 115Tb/s Transport over 100 km Using Novel Ultra-Wideband Semiconductor Optical Amplifiers," *in Proc. ECOC, paper Th.PDP. A3, Gotenborg, Sweden, 2017*.
- [13] D. F. Bendimerad, A. Ghazisaeidi, J. Vuong, P. Ramantanis, A. Seck, J. Renaudier, and Y. Frignac, "Feasibility study of wide-band in-line SOA amplification for PDM-MQAM long-haul WDM transmission systems," *in Proc. ECOC, paper , London, UK, 2013*.
- [14] A. Mecozzi and R.-J. Essiambre, "Nonlinear Shannon Limit in Pseudolinear Coherent Limit," *J. Lightwave Technol.* vol. 30, no. 12, pp. 2011-2014, 2012.
- [15] R. Dar, M. Feder, A. Mecozzi, and M Shtaif, "Inter-Channel Nonlinear Interference Noise in WDM Systems: Modeling and Mitigation," *IEEE J. Lightwave Technol.*, vol. 33, no. 5, pp. 1044-1053, March 2015.
- [16] A. Carena, G. Bosco, V. Curri, Y. Jiang, P. Poggiolini, and F. Forghieri, "EGN model of non-linear fiber propagation," *Optics Express*, vol. 22, no. 13 pp.16335-16362, May 2014.
- [17] P. Serena and A. Bononi, "A Time-Domain Extended Gaussian Noise Model," *IEEE J. Lightwave Technol.* vol. 33, no. 7, pp. 1459-1472, April 2015.
- [18] P. Johannisson and M. Karlsson, "Perturbation Analysis of Nonlinear Propagation in a Strongly Dispersive Optical Communication Systems," *IEEE J. Lightwave Technol.* vol. 31, no. 8, pp. 1273-1282, April 2013.
- [19] V. Curri, A. Carena, P. Poggiolini, G. Bosco, and F. Forghieri, "Extension and validation of the GN model for non-linear interference to uncompensated links using Raman amplification," *Optics Express Vol. 21, no. 3, pp. 3308-3317, 2013*.
- [20] G. P. Agrawal, N. A. Olsson, "Self-phase modulation and spectral broadening of optical pulses in semiconductor laser amplifiers," *J. Quantum Electron.*, vol. 25, no. 11, pp. 2297 - 2306, 1989.
- [21] M. J. Connelly, "Wide-Band Steady-State Numerical Model and Parameter Extraction of a Tensile-Strained Bulk Semiconductor Optical Amplifier," *J. Quantum Electron.*, vol. 43, no. 1, pp. 47-56, 2007.
- [22] J. Mork, and A. Mecozzi, "Theory of the ultrafast optical response of active semiconductor waveguides," *JOSAB*, vol.13, no. 8, pp. 1803-1816, 1996.
- [23] D. Cassioli, S. Scotti, and A. Mecozzi, "A time-domain computer simulator of the nonlinear response of semiconductor optical amplifiers," *J. Quantum Electron.*, vol. 36, no. 9, pp. 1072-1080, 2000.
- [24] C. Antonelli, A. Mecozzi, W. Li, and L. A. Coldren, "Efficient and Accurate Modeling of Multiwavelength Propagation in SOAs: A Generalized Coupled-Mode Approach," *J. Lightwave Technol.*, vol. 34, no. 9, pp. 2188-2197, 2016.
- [25] A. Ghazisaeidi, F. Vacondio, A. Bononi, and L. A. Rusch, "SOA Intensity Noise Suppression in Spectrum Sliced Systems: A Multicanonical Monte Carlo Simulator of Extremely Low BER," *J. Lightwave Technol.*, vol. 27, no. 14, pp. 2667-2677, 2009.
- [26] A. Ghazisaeidi, F. Vacondio, and L. A. Rusch, "Filter Design for SOA-Assisted SS-WDM Systems Using Parallel Multicanonical Monte Carlo," *J. Lightwave Technol.*, vol. 28, no. 1, pp. 79-90, 2010.
- [27] A. Ghazisaeidi, and L. A. Rusch, "Capacity of SOA-Assisted SAC-OCDMA," *Photonic Technol. Lett.*, vol. 22, no. 7, pp. 441-443, 2010.
- [28] A. Ghazisaeidi, F. Vacondio, A. Bononi, and L. A. Rusch, "Bit Patterning in SOAs: Statistical Characterization Through Multicanonical Monte Carlo Simulations," *J. Quantum Electron.*, vol. 46, no. 4, pp. 570-578, 2010.
- [29] A. Ghazisaeidi, and L. A. Rusch, "On the Efficiency of Digital Back-Propagation for Mitigating SOA-Induced Nonlinear Impairments," *J. Lightwave Technol.*, vol. 29, no. 21, pp. 3331-3339, 2011.
- [30] S. Amiralizadeh, A. T. Nguyen, C. S. Park, A. Ghazisaeidi, and L. A. Rusch, "Experimental Validation of Digital Filter Back-propagation to Suppress SOA-induced Nonlinearities in 16-QAM," *in Proc. Optical Fiber Conference, Paper OM2B.2, 2013*.